Metallurgical and Materials Engineering *Scientific paper*
Association of Metallurgical Engineers of Serbia AMES *UDC: xxxxxxx*

INVESTIGATION INTO THE KINETIC BEHAVIOR OF MOLTEN ALUMINUM PRESSURELESS INFILTRATION INTO SiC PREFORMS

Hassan Sharifi[*1], *Mohamad Reza Nasresfahani*[2]

[1] *Corresponding Author: Department of Materials Science, Faculty of Engineering, University of Shahrekord, Shahrekord, Iran*
[2] *Department of Materials Engineering, Najafabad Branch, Islamic Azad University, Najafabad, Iran (mr_nasr2001@ma.iut.ac.ir)*

Received 10.06.2016
Accepted 06.08.2016

Abstract

Infiltration of molten metal into the ceramic performs without using external force is a new fabrication method for metal-matrix composites. In this research, the kinetics of pressureless infiltration in the processing of Al/SiC composites has been investigated. In order to improve the wettability and infiltration properties, Al-6wt.%Mg alloy was prepared. Also, the ceramic component was coated with electroless copper plating at the temperature 60-70 °C (pH=12.5) and the rate of 17-20 µm. Infiltration of molten aluminum into the coated ceramic perform was successfully carried out in the temperature range of 850 to 950 °C under nitrogen atmosphere. Microstructural SEM investigations indicated a well-bonded metal-ceramic joint. Kinetic studies showed that the melt infiltration into the ceramic foam follows an S-shaped curve. The infiltration rate was specified with respect to variables like the experiment temperature and the size of the porosities of the ceramic component. The results revealed that by increasing the temperature and the size of pores, the infiltration rate increases. For infiltrating molten metal into the 10 and 30 ppi foams, activation energies of 5.902 kJ/mol and 7.232 kJ/mol, are required, respectively.

Keywords: Kinetic, Aluminum Composite, Silicon carbide, Pressureless Infiltration.

Introduction

Metal matrix composites exhibit higher elastic modulus, higher strength, better high temperature performance, less weight, lower thermal expansion coefficient and a

* Corresponding author: Hassan Sharifi, sharifi@eng.sku.ac.ir

higher wear resistance compared with monolithic metals and alloys [1, 2]. Since the volume fraction and continuity of the reinforcing phase affect the mechanical and physical properties of the composites, it is of importance to control the distribution and the amount of the reinforcing phase in the processing of metal matrix composites. [3]. Metal matrix composites are commonly reinforced with ceramic materials and intermetallic compounds including Al_2O_3, SiC, ZrO_2, B_4C, Si_3N_4 [4].

Metal matrix composites' production routes can be classified into liquid, solid and semi-solid state processes [5]. Liquid state processes include melt stirring, in situ processing, spray processing, melt infiltration and centrifuge casting [6]. The melt infiltration process results in products of high quality with dimensions close to the final product. Therefore, this method is widely used. Common infiltration methods include [7-10]: a) infiltration under an external pressure (squeeze casting [11] and infiltration with gas pressure [12, 13]), b) infiltration under vacuum [14] and c) infiltration without an external pressure (pressureless). First introduced by Aghajanian et al. [15, 16], the pressureless infiltration (automatic infiltration process) is a suitable, low cost method for production of composites. They reported that molten metal can be infiltrated into a porous ceramic without an external pressure and by controlling the chemical composition of the alloy. The porous ceramic is made of a powder substrate, foam or pre-form with controlled volume fraction of the cavities. Aghajanian et al. for the first time infiltrated the aluminum alloy into an Al_2O_3 and SiC powder substrate under controlled atmosphere without pressure [15, 16].

In recent years much attention has focused on the production of three-dimensional network structure metal matrix composites (3DNMMCs) through pressureless infiltration. Composites like Al-Al_2O_3 [15], Al-Al_2O_3+SiC [16], Al-Si_3N_4[17], Al-SiC[21-18], Al-BN[22], Al-Zn/SiC[23], Mg/SiC[24] and Al/B_4C[25] have been produced by this method.

One of the major challenges when processing metal matrix composites is achieving the highest wettability. Wetting is the ability of a liquid to coat a solid surface. Among different methods used for measuring wettability of ceramics by liquid metals, the sessile-drop method is the most famous one [26]. In a metal-ceramic system, the contact angle depends on the thermodynamics as well as the kinetics of the reactions. When infiltrating the liquid metal into the ceramic preform, a period of time called Latency time, is required [27]. This is because of the oxide layer on the surface of the molten metal.

The aim of the present study is to investigate the kinetics of pressureless infiltration of liquid aluminum into SiC preforms. The effects of pore size and temperature of the liquid metal on the infiltration rate have also been studied.

Experimental design and materials

In this research, SiC ceramic foams of 10 and 30 Pores Per Inch (PPI) were used to form a cylinder of 20 mm diameter and 80 mm height. These open porosity type of foams are made in Lanik Foam Ceramic Company [28]. A copper film was electroless plated on SiC foam to improve the wettability of the melt with the foam. Before coating, the foams were sensitized for 15 minutes in a solution (30ml/lit HCl+10 gr/lit $SnCl_2.2H_2O$) and activated for 20 minutes in a solution (25ml/lit HCl+$PdCl_2$). The samples were then washed with distilled water and copper coated. The chemical

composition of the copper bath is given in Table 1. The optimal coating conditions were obtained at 60-70 °C, pH=12.5 by the rate of 17-20 µm for 20 minutes. In this study, Al-6%Mg alloy was used as the matrix. The alloy smelting process and the alloying were done by using an induction furnace [29].

Table 1. Chemical composition of the copper bath.

Copper(II) Sulfate, Pentahydrate	$CuSO_4.5H_2O$	8g/L
EDTA, disodium salt	$C_{10}H_{14}O_8N_2Na_2.2H_2O$	32g/L
2,2'-Dipyridyl	$C_{10}H_8N_2$	20g/L
Potassium hexacyanoferrate(II)	$K_4Fe(CN)_6.3H_2O$	60g/L
Formaldehyde, 37%solution	HCHO	7g/L

In order to produce the Al-6%Mg/SiC composite, the SiC preform was placed in a cylindrical alumina crucible and the alloy ingot was placed on the top of the foam. Several titanium sheets were then placed around the crucible to deoxygenate the furnace gas. After sealing the furnace, by using a vacuum pump, the pressure inside the furnace was reduced to 10^{-4} Pa and nitrogen gas was then injected into the furnace. The heating rate of the furnace was 20 ºC/min and the infiltration was performed at 850-950 ºC. After infiltration, the furnace was turned off but nitrogen injection continued up to 500 ºC. By reaching the room temperature, the door of the furnace was opened and the composite samples were taken out. The infiltration length in the ceramic foams was measured with respect to the infiltration time. Samples were examined by light microscopy and scanning electron microscopy (SEM).

Discussion

Macroscopic examination

Ceramic properties provided a continuous and uniform distribution of reinforcements in metal matrix composites. The uniform distribution of reinforcements improves the mechanical properties of the composites. Fig.1 shows macroscopic images of Al-6Mg/SiC composites prepared with foams of different pore sizes.

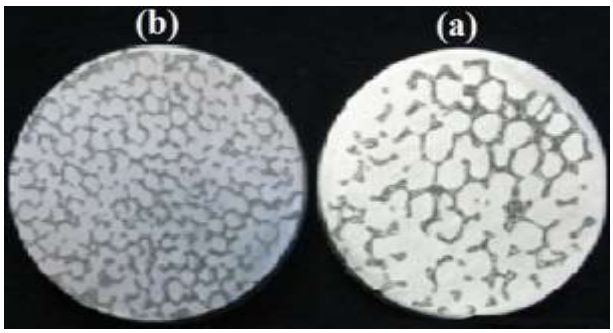

Fig. 1. Macroscopic images of Al-6Mg/SiC composites infiltrated at 900 ºC into ceramic preforms with different pore size: a) 10 ppi and b) 30 ppi

In this figure, the dark areas are SiC reinforcements and the bright areas represent the aluminum alloy. Macroscopic examination of samples in the temperature range of 850-950 ºC did not show any impermeability or porosity. From a macroscopic aspect, the molten aluminum alloy completely infiltrates into the porosities. Fig. 2 shows a microscopic image of the produced composite using the 30 ppi foam.

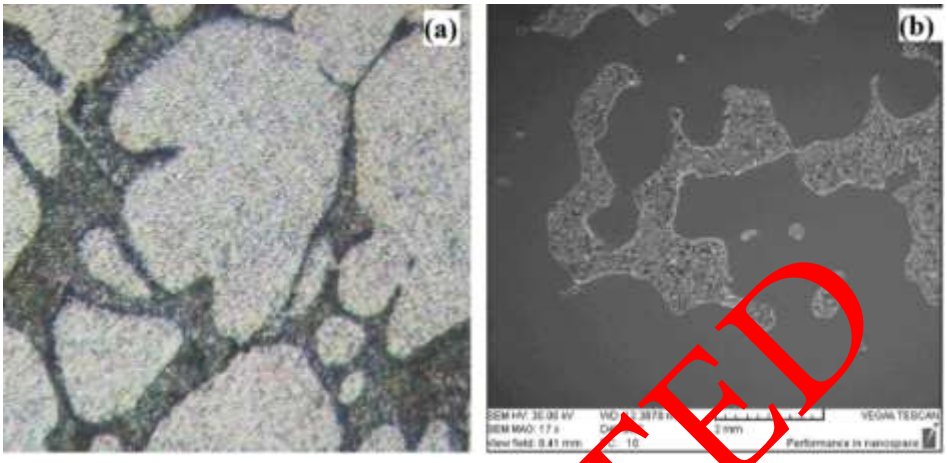

Fig. 2. Microscopic images of Al-6Mg/SiC(30ppi): a) optical microscopy and b) scanning electron microscopy.

Infiltration kinetic

Infiltration measurement

The infiltration length of molten metal in the ceramic foam, using composite cross-sections, was determined as a function of time and temperature. This study shows that coating the ceramic with a copper film can increase the infiltration length. The melt front in the ceramic channels of incompletely infiltrated samples has a curved surface. Therefore, the required force for infiltration can be measured by using the Young-Laplace equation [30]:

$$\Delta P = \frac{2\gamma_{lg}\,Cos\theta}{r} \qquad (1)$$

Where γ_{lg}, θ, r and ΔP are the surface energy of the melt, the wetting angle, the average size of the channels of a pre-ceramic and the needed pressure for infiltration, respectively. To have an improved infiltration, the required force for infiltration can be reduced. This reduction depends on the dimensions of the channels in the foam, the pressure of the liquid weight at the top of the foam, the interaction of the alloying elements Mg, N_2 and the reaction of the liquid with the ceramic coating.

The presented model in Fig. 3 describes how the melt is infiltrated into the ceramic foam. As shown in Fig. 3, in early stages of infiltration, θ angle (at the melt front) is greater than 90 degrees and the surface curvature of the melt is outward. This is because of the existence of an oxide layer on the surface of the melt which prevents

penetration into the channels. Due to the interaction between alloying elements of the melt, atmosphere of the furnace and ceramic coating, the oxide layer is dissolved and θ is reduced (Fig. 3b). In these circumstances, the infiltration resistance decreases. Finally, θ is less than 90 degrees, the orientation of the melt curvature changes and the infiltration begins (Fig. 3c).

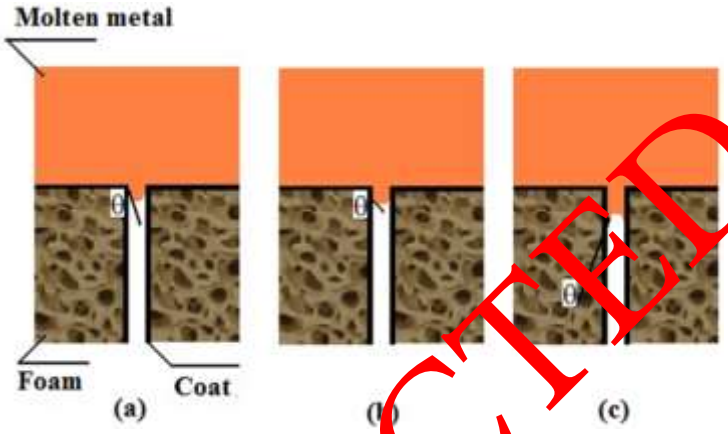

Fig. 3. Schematic of infiltrated molten metal into the ceramic pre-form.

Fig. 4 shows the infiltration length as a function of temperature for the Al-6Mg/SiC composite. These are the average values from several sections of measured samples. The graphs in Fig. 4 show that the infiltration length substantially increases by increasing the melt temperature due to the reduction in surface energy and the reaction between the melt and the copper film.

This contributes to the reduction in the contact angle and results in an improved infiltration. Infiltration operations are intensified by an exothermic reaction at the liquid-solid interface which produces intermetallic compounds of aluminum and copper. Each of the graphs in Fig. 4 can be divided into three distinct areas: the latency area, the quick infiltration area, and the stable area. It is seen that by increasing the temperature, the latency period (the time required for the start of infiltration) is shortened while the infiltration rate is increased. The quick infiltration area starts quickly after the latency period and becomes a stable area at the end. It can be concluded that regardless of the temperature and the size of the pores, the infiltration graphs follow an S-shaped parabolic curve. This has also been reported by other researchers. Wang et al. infiltrated liquid Al-5 wt.% Mg into a Si_3N_4 pre-ceramic at 850, 950 and 1050 ºC under an argon atmosphere. They reported that pressureless infiltration is a kinetic process during which the infiltration time is reduced by increasing the melt temperature. Based on their results, at all temperatures, the infiltration length is a function of time and this relationship follows an S-shaped parabolic curve [30]. Carlos et al. infiltrated molten aluminum into SiC particles coated with nickel at 800, 850 and 900 ºC. They also confirmed that the relationship between infiltration length and time follows an S-shaped parabolic curve [31].

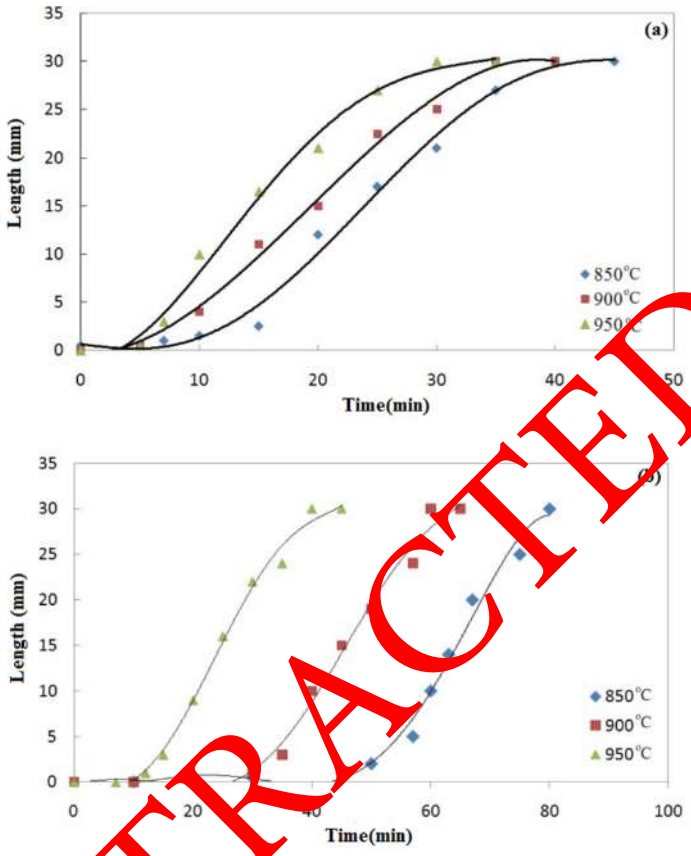

Fig. 4. The infiltration length of molten Al-6Mg into SiC preforms of different pore size: a) 10 ppi, b) 30 ppi

According to Fig. 4, there is a direct relation between the pore size and the infiltration length. In same conditions and for a 30 ppi foam, the time effect is larger compared to the 10 ppi foam. In fact, by increasing the size of the pores in the foam, the infiltration rate increases. One of the most important parts of these graphs is the latency time before matching them with a parabolic curve. However, the latency time decreases by increasing the temperature. On the other hands, the latency time is reduced when decreasing ppi due to the reduction in the contact area between the ceramic and molten alloy and breakdown of the oxide film.

Infiltration rate

Fig. 5 shows the relationship between the squared infiltration length (l^2) and time (t) for Al-6 wt.% Mg/SiC composite.

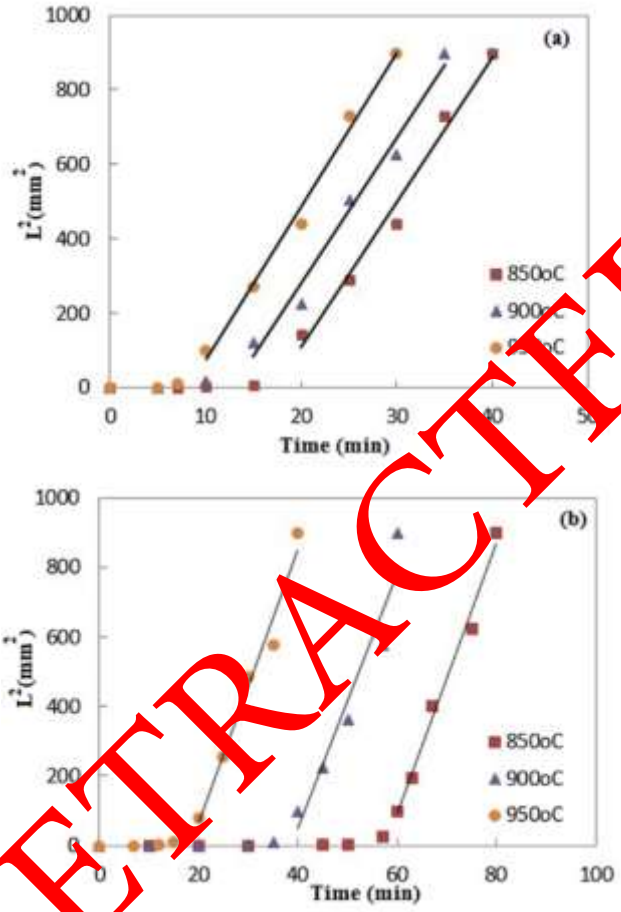

Fig. 5. Squared infiltration length of molten Al-6Mg into SiC performs of different pore size: a) 10 ppi, b) 30 ppi.

According to these graphs, there is a linear relation between them which means the infiltration condition is stable. Thus, it can be stated that:

$$l^2 = Kt \qquad (2)$$

Here K is a parabolic constant, achieved by regression of l^2-t graph slope.

To calculate the infiltration rate, Eq. 2 was derived with respect to time. So the infiltration rate at 50% of infiltration is expressed by Eq. 3:

$$(dl/dt) = \frac{K^{1/2}}{2(t^{1/2})_{50\%}} \qquad (3)$$

By using Eq. 2, one can write:

$$(t^{1/2})_{50\%} = \frac{l_{50\%}}{K^{1/2}} \tag{4}$$

$$l_{50\%} = \frac{1}{2} \tag{5}$$

Eq. 6 is achieved by combining Eqs. 3 to 5:

$$(dl/dt)_{50\%} = \frac{K}{l} \tag{6}$$

By inserting (K) and (l) into Eq. 6, the infiltration rate was calculated and presented in Table 2. The obtained values indicate that the infiltration rate increases by increasing the temperature and decreasing the ppi of the foam. It is seen that by reducing the ppi of the foam, K is increased and the infiltration kinetic is improved.

If the viscosity resistance of the melt flow into the ceramic foam is considered as a capillary flow, the Poiseuille law can be written as following [32]:

$$\frac{dV}{dt} = \frac{\pi r^4 \Delta P}{8\eta l} \tag{7}$$

Where, ΔP is the pressure differential which forces the melt flow into the capillary channels; η is dynamic viscosity; and *dV/dt* is volumetric flow rate. By considering $dV = \pi r^2 dl$ and Eq. 1, one can write:

$$l^2 = \left[\frac{r\gamma_{lv}\cos\theta}{2\eta}\right] t \tag{8}$$

The above statement shows that by increasing the (r), the melt flow into the porous foam increases and the kinetic of infiltration is improved. Note that, Eq. 8 offers a simple expression of infiltration. As shown in Table 2 the infiltration rate increases by increasing the temperature.

Table 2. The infiltration length parameters.

Pores per inch (ppi)	Temperature (°C)	K (m^2/s)	Infiltration rate (mm/s)
10	800	39.03	1.301
	900	39.16	1.305
	950	41.14	1.371
30	800	36.75	1.225
	900	38.75	1.291
	950	39.16	1.305

An Arrhenius analysis can be imposed on the graphs of Fig. 4. The results are shown in Fig. 6. In this figure, the slope of the line represents the activation energy of infiltration which is related to the infiltration through an Arrhenius equation:

$$(dl / dt) = A \exp(\frac{E_o}{RT}) \qquad (9)$$

Where, (A) is a constant number and (R) is the universal gas constant. The calculated activation energy for infiltrating the molten Al-6Mg into 10 and 30 ppi SiC foams are 5.902 (kJ/mol) and 7.232 (kJ/mol), respectively. The results show that by reducing the ppi of the foams the activation energy decreases.

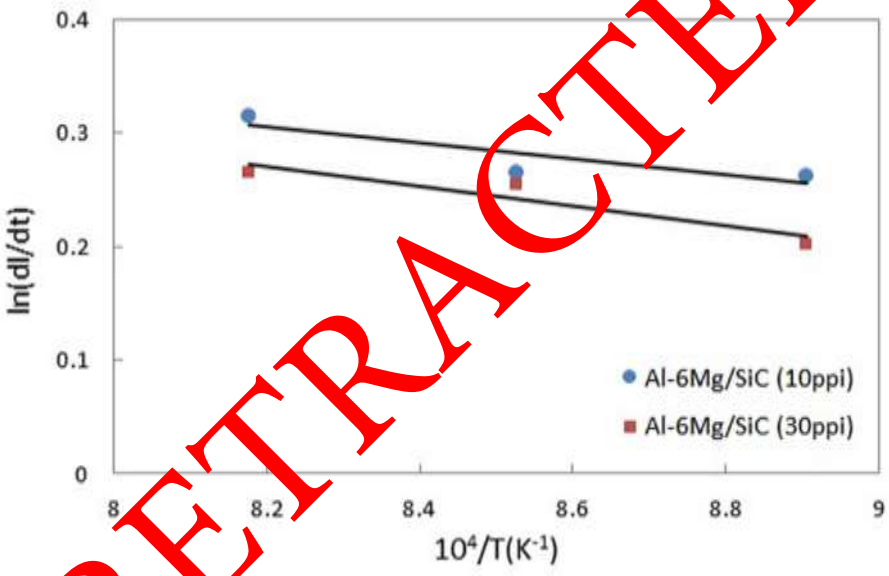

Fig. 6. Arrhenius graph of infiltration rate of molten Al-6Mg into SiC perform.

Latency mode

The latency time is defined as the required time for the start of infiltration. As shown in Fig. 4, the latency time is decreased by increasing the temperature and decreasing the ppi of the foam. In fact, the latency time represents the time needed for the molten surface oxides to be broken and let the infiltration improve. Thermodynamic calculations using the HSC software showed that Mg/ melt oxide layer and molten metal/ceramic coating reactions at a temperature range of 850-950 °C are probable and will improve infiltration. The latency time depends on the size of the pores of the foamed ceramic. For the foams with higher ppi (smaller size of the pores), this time will be longer. In fact, the decrease in the pore size causes an increase in the contact area of the foam with molten aluminum alloy. Therefore, the latency time is increased in the presence of surface oxides.

Conclusion

Molten aluminum alloy infiltration into SiC foam is possible by controlling the chemical composition of the melt and atmosphere. Also, the copper coating on the ceramic component improves the connection between the molten Al-6Mg and SiC at the interface. Regardless of the infiltration temperature and the size of the pores of the pre-ceramic, the infiltration graphs are parabolic S-shaped. It was observed that by increasing the temperature as well as the size of the pores in the pre-ceramic, the infiltration rate increases. Activation energy is also required for the start of infiltration and is increased by decreasing the size of the pores.

References

[1] K.U. Kainer, Metal Matrix Composites, Custom-made materials for automotive and aerospace engineering, first ed.,Wiley-Vch Press, 2003.
[2] J. Eliasson, R Sandstrom: Key Eng Mater, 36 (1995) 104-107.
[3] W. Shou-ren, G. Hao-ran, W. Ying-Zi,: J Mater Sci, 41 (2006) 6751-5757.
[4] J.W. Kaczmar, K. Pietrzak, W. Wlosinski: J Mater Process Technol, 106 (2000) 58-67.
[5] S. Vaucher, J. Kuebler, O. Beffort, L. Biasetto, F. Zordan, P. Colombo: Compos Sci Technol, 68 (2008) 3202–3207.
[6] M. Mizumoto, T. Ohgai, A. Kagawa: J Mater Sci Eng A, 413–414 (2005) 521–526.
[7] E. Akbarzadeh, A.P Josep, M. Picas, B. Teresa: Mater Des, 88 (2015) 683–692.
[8] S. Ren, X. Qu, X. He, M. Qin, X. Shen: J Alloys Compd, 484 (2009) 256-262.
[9] J. Liu, Z. Zheng, J. Wang: J Alloys Compd, 465 (2007) 239-243.
[10] G. Kraub, J. Kubler, E. Trentini: J Mater Sci Eng A, 337 (2002) 315-322.
[11] S.N. Chou, J.L. Huang, D.F. Lii, H.H. Lu: J Alloys Compd, 419 (2006) 98-102.
[12] A. Demir, N. Altinkok: Compos Sci Technol, 64 (2004) 2067-2074.
[13] E. Carreno-Marelli, T. Cutard, R. Schaller, C. Bonjour: J Mater Sci Eng A, 251 (1998) 48-57.
[14] Y. Shahin, M. Acilar: Composites, Part A, 34 (2003) 709-718.
[15] M.K. Aghajanian, N.H. Macmillan, C.R. Kennedy, S.J. Luszcz, R. Roy: J Mater Sci, 24 (1989) 58-670.
[16] M.K. Aghajanian, M.A. Rocazella, J.T. Burke, S.D. Keck: J Mater Sci, 26 (1991) 447-454.
[17] K.B. Lee, H. Kwon: Metall Mater Trans A, 30A (1999) 2999-3007.
[18] A.M. Zahedi, H.R. Rezaie, J. Javadpour, M. Mazaheri, M.G. Haghighi: Ceram Int, 35 (2009) 1919-1926.
[19] X. Shen, S. Ren, X. He, M. Qin, X. Qu: J Alloys Compd, 468 (2009) 158-163.
[20] J.A. Aguilar-Martinez, M.B. Hernandez, J. Castillo-Torres, M.I. Pech-Canul: Rev Mex Fis, 53 (2007) 205-209.
[21] [J.A. Aguilar-Martinez, M.I. Pech-Canul, M. Rodriguez-Reyes, J.L. De la Pena: J Mater Sci, 39 (2004) 1025-1028.
[22] K.B. Lee, J.P. Ahn, H. Kwon: Metall Mater Trans A, 32A (2001) 1007-1018.
[23] K.B. Lee, H. Kwon: Metall Mater Trans A, 33A (2002) 455-465.
[24] V. Kevrkijan: Metall Mater Trans A, 35A (2004) 707-715.
[25] I. Kerti, F. Toptan: Mater Lett, 62, (2007) 1215-1218.

[26] S.Y. Oh, J.A. Cornie, K.C. Russell: Metall Mater Trans A, 20A (1989) 527-531.
[27] S.F. Corbin, X. Zhao-jie, H. Henein, P.S. Apte: J Mater Sci Eng A, 262 (1999) 192–203.
[28] H. Sharifi, M. Divandari, A.R. Khavandi, M.H. Idris: Acta Metall Sin, 23 (2010) 1-7.
[29] H. Sharifi, A.R. Khavandi, M. Divandari, M.I. Hasbullah: Int J Miner, Metall Mater, 19 (2012) 77-82.
[30] S.R. Wang, Y.Z. Wang, Q. Chi: J Mater Sci, 42 (2007) 7812-7818.
[31] C.A. Leon-Patino, R.A.L. Drew: Curr Opin Solid State Mater Sci, 9 (2005) 211–218.
[32] D. Lee, S.W. Park, D.B. Lee: Met Mater Int, 14 (2008) 419-423.